

Non-thermal dark matter production and leptogenesis in a $L_\mu - L_\tau$ model

XinXin Qi, Hao Sun

Institute of Theoretical Physics, School of Physics, Dalian University of Technology, No.2 Ling-gong Road, Dalian, Liaoning, 116024, P.R.China

E-mail: qxx@mail.dlut.edu.cn, haosun@dlut.edu.cn

ABSTRACT: We discuss the possibility of light scalar dark matter generated by right-handed neutrino in a $L_\mu - L_\tau$ model, in which the dark matter ϕ_{dm} carries $U(1)_{L_\mu-L_\tau}$ charge but it is a singlet in the Standard Model. We discuss the case that dark matter production mainly comes from scattering associated with a pair of right-handed neutrinos non-thermally while other related processes are highly suppressed. A feasible parameter space is considered and we found the correct dark matter relic density can be obtained without influencing the result of leptogenesis result. The heavier right-handed neutrino will induce colder dark matter production and the allowed dark matter mass region is $[10^{-5} \text{ GeV}, 0.1 \text{ GeV}]$.

Contents

1	Introduction	1
2	Model description	3
3	muon g-2	5
4	Dark matter from leptogenesis	6
4.1	Leptogenesis	7
4.2	Dark matter	10
4.3	Combined results	13
5	summary	16

1 Introduction

The Standard Model (SM) is regarded as one of the most successful theories in physics, which can describe strong and electroweak interactions in an elegant way. However, there are still other open questions the SM can not explain. Neutrino oscillation experiments [1, 2] indicate that neutrinos are not massless, and the mass of neutrinos are at the sub-eV level, which is contrary to the SM. According to astronomical exploration, our universe is not only composed of baryon matter, but also composed of dark matter (DM) and dark energy. The combined analysis shows that the dark matter density and baryon density are [3]:

$$\Omega h^2 = 0.12 \pm 0.001 \text{ and } \Omega_b h^2 = 0.0224 \pm 0.0001, \quad (1.1)$$

respectively. In addition, the number of baryons in the universe is not equal to the number of anti-baryons. The baryon asymmetry can be expressed by [3]:

$$\eta \equiv \frac{n_B - n_{\bar{B}}}{n_\gamma}|_0 = (6.12 \pm 0.03) \times 10^{-10} \quad (1.2)$$

or

$$Y_B \equiv \frac{n_B - n_{\bar{B}}}{s}|_0 \approx 8.7 \times 10^{-11} \quad (1.3)$$

where n_B , $n_{\bar{B}}$, n_γ and s are the number densities of baryons, anti-baryons, photons and entropy, respectively. The subscript 0 means at present time.

The evidence of neutrino mass, dark matter and baryon asymmetry in the universe provide us with new hints beyond SM. In particular, by introducing right-handed neutrinos, the problems of neutrino mass and baryon asymmetry can be solved simultaneously

with leptogenesis [4], where the light neutrino mass can be generated via the type-I seesaw mechanism [5–9], and the decays of right-handed neutrinos in the early universe can produce the baryon asymmetry naturally. Concretely speaking, a lepton asymmetry can be generated through the CP-violating and out-of-equilibrium decay of right-handed neutrinos in the early universe during leptogenesis, and this asymmetry can be converted into baryon asymmetry via $(B + L)$ -violating interactions during the electroweak symmetry breaking (EWSB) phase transition.

Attempts at models relating dark matter to baryon asymmetry have been discussed in Refs.[10–33], and among these models a two sector leptogenesis scenario is introduced to produce comparable baryon and dark matter number densities based on the fact of $\Omega h^2 \approx 5\Omega_b h^2$. Such a scenario connects dark matter and leptogenesis together, in which the heavy right-handed neutrinos couple to the dark sector as well as the SM leptons in the visible sector, which results in an asymmetry in both dark and visible sectors simultaneously. Typically, as discussed in Refs.[34, 35], the two-sector leptogenesis scenario can also relate light dark matter with leptogenesis and predicts light dark matter mass ranging from keV to GeV without matching asymmetries between visible and dark sector. Imitating a similar idea, we assume SM particles and dark matter are related via Yukawa interactions to the same right-handed neutrinos, and the right-handed neutrinos provide a common origin of the light neutrino mass (type-I seesaw mechanism), leptogenesis (decay of heavy right-handed neutrinos related with CP violation) and dark matter (heavy neutrinos generate dark matter via Yukawa interactions).

In principle, the shared production mechanism to generate baryon asymmetry and the dark matter relic density in our universe often demands adding new particles to the SM. For example, the additional Yukawa terms can connect right-handed neutrinos and dark matter with an extra scalar field which is SM singlet. Such singlet scalar field can be unified in concrete models and introduce new phenomenology at the LHC experiments. One of the most attractive models including such new scalar fields is $L_\mu - L_\tau$ extension of the SM [36–45], which involves a new gauge boson Z_p , and a singlet scalar with $L_\mu - L_\tau$ charge. The new light gauge boson Z_p can explain the $(g - 2)_\mu$ anomaly [46–48] naturally considering the one-loop contribution of Z_p to muon’s magnetic dipole momentum [41]. Discussion about dark matter in the $L_\mu - L_\tau$ model can be found in Refs.[49–56] while leptogenesis in the $L_\mu - L_\tau$ model can be found in Refs.[57–59].

In this work, we consider dark matter carries $U(1)_{L_\mu - L_\tau}$ charge and is a singlet in the SM. We discuss the possibility of non-thermal dark matter production generated by right-handed neutrinos at the early universe, which contributes to the observed dark matter relic density. What’s more, we focus on the relic density constraint on the parameter space of scatterings within the non-thermal mechanism. For the above issues, we have the following comments: Firstly, the dark matter ϕ_{dm} has several production channels: gauge portal, Higgs portal and Yukawa portal. For the Higgs portal, one can fine-tune the scalar-DM couplings to be relatively small so that the contribution of the Higgs portal channels to dark matter production can be negligible. For the gauge portal, dark matter carries $U(1)_{L_\mu - L_\tau}$ charge and a high scale breaking $L_\mu - L_\tau$ symmetry is considered, which leads to a tiny $U(1)_{L_\mu - L_\tau}$ charge of dark matter, and the gauge portal contribution will

be highly suppressed due to the choice of the small charge. Therefore, Yukawa portal channels can play an important role in determining dark matter abundance. Note that right-handed neutrinos can not only generate the baryon asymmetry via the leptogenesis mechanism but also dark matter simultaneously in the model. On the other hand, there can be no dark matter initially and dark matter particles can be produced through the decay or annihilation of heavier particles (right-handed neutrinos in this work) that were present in the early Universe, and the non-thermal production can contribute to the dark matter abundance. Unlike most two-sector leptogenesis scenarios, where sterile neutrinos as dark matter are coupled to the scalar field in the dark sector and right-handed neutrinos through the Yukawa term and the dark matter abundance is derived through the decays of right-handed neutrinos during the leptogenesis process [34]. In this work, we consider a scheme in which a singlet scalar is the dark matter coupling directly to the right-handed neutrinos. Furthermore, the abundance of dark matter is mainly given by the scattering process during leptogenesis, which leads to dependence of the dark matter abundance with the singlet Yukawa interactions instead of the branching ratio[60].

The article is arranged as followed, in section 2, we give the scalar dark matter model based on the $L_\mu - L_\tau$ framework. In section 3, we briefly discuss the $(g - 2)_\mu$ anomaly in the model. In section 4, we discuss the dark matter phenomenology as well as leptogenesis in the model, and finally we summarize in the last section of the paper.

2 Model description

In the context of the minimal $L_\mu - L_\tau$ model with only one extra singlet scalar [58, 59], the $\mu\mu$ and $\tau\tau$ entries of the right-handed neutrino mass matrix are equal to zero, which leads to a so-called two-zero minor structure [43] in the light neutrino mass matrix. According to the global fit data [61–63] and cosmology constraints [3] on the sum of light neutrino masses, it is difficult to satisfy the data in such a minimal model as discussed in Refs.[43, 59]. In this work, we consider one possible extension of the minimal $L_\mu - L_\tau$ model [64] including scalar dark matter ϕ_{dm} as followed in Table 1.

Gauge group	Fermion Fields			Scalar Field			
	N_e	N_μ	N_τ	H_2	H_3	$\phi_{1,2}$	ϕ_{dm}
$SU(2)_L$	1	1	1	2	2	1	0
$U(1)_Y$	0	0	0	1/2	1/2	0	1
$U(1)_{L_\mu-L_\tau}$	0	q	$-q$	$1 - q$	$-1 + q$	$q, 2q$	$2q$

Table 1. New Particles and their respective gauge charges in the non-minimal model.

We introduce three right-hand neutrinos N_e , N_μ and N_τ to the SM, and the corresponding $U(1)_{L_\mu-L_\tau}$ charge are 0, q and $-q$ respectively, where q is a certain number. We also introduce two doublet scalar fields H_2 and H_3 with $U(1)_{L_\mu-L_\tau}$ charge $1 - q$ and $q - 1$ as well as two singlet scalars with $U(1)_{L_\mu-L_\tau}$ charge q and $2q$, the singlet scalar dark matter ϕ_{dm} charge is $2q$.

Lagrangian related with neutrino mass as well as dark matter can be written as:

$$\begin{aligned}
\mathcal{L} \supseteq & -y_{sm}\phi_{dm}N_\mu N_\mu - y_{st}\phi_{dm}^\dagger N_\tau N_\tau - \frac{M_{\mu\tau}}{2}N_\mu N_\tau - \frac{M_{ee}}{2}N_e N_e - y_{e\mu}\phi_1^\dagger N_e N_\mu - y_{e\tau}\phi_1 N_e N_\tau \\
& - y_\mu\phi_2^\dagger N_\mu N_\mu - y_{D_e}\bar{L}_e\tilde{H}N_e - y_{D_\mu}\bar{L}_\mu\tilde{H}_2N_\mu - y_{D_\tau}\bar{L}_\tau\tilde{H}_3N_\tau - y_\tau\phi_2N_\tau N_\tau - y_{le}\bar{L}_e H e_R \\
& + y_{l\mu}\bar{L}_\mu H \mu_R + y_{l\tau}\bar{L}_\tau H \tau_R + \text{h.c.}, \tag{2.1}
\end{aligned}$$

where $\tilde{H} = i\sigma_2 H$, $\tilde{H}_2 = i\sigma_2 H_2$ and $\tilde{H}_3 = i\sigma_2 H_3$. There are three Higgs doublets and two SM singlets in such model, and the scalar doublet H plays the role of SM Higgs. We focus on the interplay between the dark matter and leptogenesis while the couplings of dark matter with other scalar fields such as $|\phi_{dm}|^2|H|^2$ are negligible. On the other hand, ϕ_{dm} can have quadratic and trilinear terms with other singlet scalars such as $\phi_1^2\phi_{dm}^\dagger, \phi_{dm}^\dagger\phi_2$, which should be fine-tuning to satisfy dark matter lifetime bound. For simplicity, we set these couplings to be zero. The doublets will be massless at the scale of leptogenesis because of the unbroken electroweak symmetry, while the singlet scalars are massive since the scale of $U(1)_{L_\mu-L_\tau}$ symmetry breaking is above the leptogenesis scale in the model. Although the singlet scalars play no role in leptogenesis, their masses are constrained by LHC experiments due to the mixings with SM like Higgs boson [65, 66]. The most stringent constraint on the mixing angle θ arises from the W boson mass correction [67] at NLO with $0.2 \lesssim \sin\theta \lesssim 0.3$ in the case of $250 \text{ GeV} \lesssim m_{\phi_i} \lesssim 850 \text{ GeV}$, where m_{ϕ_i} is the mass of the singlet scalar ϕ_i . For $m_{\phi_i} < 250 \text{ GeV}$, the LHC and LEP direct search [68, 69] and measured Higgs signal strength [69] yield $\sin\theta \lesssim 0.25$. For $m_{\phi_i} > 850 \text{ GeV}$, we have $\sin\theta \lesssim 0.2$ from the requirement of perturbativity and unitarity. In summary, the bounds are mild for $m_{\phi_i} < 1 \text{ TeV}$. Since the singlet scalars make no difference in leptogenesis, the mixing angle can remain as small as required by tuning their couplings with SM like Higgs. On the other hand, the physical scalars from the Higgs doublets are also constrained by experiments. Similar with the singlet scalar case, we can satisfy these bounds by tuning the related parameters and without changing the results about leptogenesis. In this work, we don't elaborate on them further.

For simplicity, we assume the vevs of these scalar fields are given by,

$$\langle H \rangle = v_0, \quad \langle H_2 \rangle = \langle H_3 \rangle = v_h, \tag{2.2}$$

$$\langle \phi_1 \rangle = \langle \phi_2 \rangle = v_b \tag{2.3}$$

and we have,

$$v_0^2 + 2v_h^2 = 246^2, \quad M_{Z_p} = \sqrt{5}g g_p v_b \tag{2.4}$$

After spontaneous symmetry breaking, the right-handed neutrino mass matrix and Dirac neutrino mass matrix are given by,

$$M_R = \begin{pmatrix} M_{ee} & y_{e\mu}\frac{v_b}{\sqrt{2}} & y_{e\tau}\frac{v_b}{\sqrt{2}} \\ y_{e\mu}\frac{v_b}{\sqrt{2}} & \sqrt{2}y_\mu v_b & \frac{M_{\mu\tau}}{2} \\ y_{e\tau}\frac{v_b}{\sqrt{2}} & \frac{M_{\mu\tau}}{2} & \sqrt{2}y_\tau v_b \end{pmatrix} \tag{2.5}$$

and

$$M_D = \begin{pmatrix} y_{De} \frac{v_0}{\sqrt{2}} & 0 & 0 \\ 0 & y_{D\mu} \frac{v_h}{\sqrt{2}} & 0 \\ 0 & 0 & y_{D\tau} \frac{v_h}{\sqrt{2}} \end{pmatrix} \quad (2.6)$$

respectively. The light neutrino mass matrix M_ν can be generated by the Type-I seesaw mechanism with

$$M_\nu = -M_D M_R^{-1} M_D^T = U^* \hat{M}_\nu U^\dagger, \quad (2.7)$$

where $\hat{M}_\nu = \text{diag}\{m_1, m_2, m_3\}$ with m_1, m_2 and m_3 being the light neutrino mass, and U is the Pontecorvo-Maki-Nakagawa-Sakata (PMNS) matrix [70, 71]. In order to simplify the following discussion, we take the following benchmark values of the PMNS matrix with [72],

$$U = \begin{pmatrix} 0.82571 & 0.82571 & -0.124534 - 0.0846333i \\ -0.354387 - 0.0454376i & 0.683844 - 0.0299151i & 0.635459 \\ 0.433147 - 0.0541505i & -0.484417 - 0.0356514i & 0.757311 \end{pmatrix} \quad (2.8)$$

For the light neutrino mass, the two distinctive neutrino mass squared differences can be given by [72],

$$\Delta m_{21}^2 = m_2^2 - m_1^2 = 7.4 \times 10^{-23} \text{ GeV}^2 \quad (2.9)$$

$$\Delta m_{31}^2 = m_3^2 - m_1^2 = 2.515 \times 10^{-21} \text{ GeV}^2 \quad (2.10)$$

3 muon g-2

In the $L_\mu - L_\tau$ model, the $(g-2)_\mu$ anomaly can be solved naturally with the Z_p one loop contribution. The analytical expression for Δa_μ is [73]

$$\Delta a_\mu = \frac{g_p^2 m_\mu^2}{8\pi^2} \int_0^1 \frac{2\omega^2(1-\omega)}{\omega^2 m_\mu^2 + (1-\omega)M_{Z_p}^2} d\omega \quad (3.1)$$

where m_μ is the muon mass. We ignore the possible contribution of the additional Higgs doublets and focus on the gauge boson Z_p as discussed in Ref. [64]. Direct searches for new gauge bosons at experiments have already given stringent constraints on the parameter space of (M_{Z_p}, g_p) . At colliders, the Z_p gauge boson can be produced via $e^+e^- \rightarrow \mu^+\mu^- Z_p$ with the subsequent decay of $Z_p \rightarrow \mu^+\mu^-$ [74]. Such a search can be found in Babar [75] and give us the possible bound on $M_{Z_p} - g_p$ plane. What's more, neutrino experiments give us new clues to constrain the parameter space [76]. The Borexino data related to the scattering of low energy solar neutrinos [77, 78] can provide the most stringent constraint on the low M_{Z_p} and low g_p region. Another constraint is from CCFR collaboration [79], obtained via the neutrino trident production where a muon neutrino scattered off of a nucleus producing a $\mu^+\mu^-$ pair. Such a process will be enhanced due to the existence of

Z_p compared with the SM case. The above experiments constrain the $g_p - M_{Z_p}$ parameter space with $M_{Z_p} \sim (10, 200)$ MeV and $g_p \lesssim 10^{-4} \sim 10^{-3}$ level. See details that are shown in Fig.1. Experiment bounds on $g_p - M_{Z_p}$ indicate qv_b in Eq. 2.4 is approximately equal to a hundred GeV.

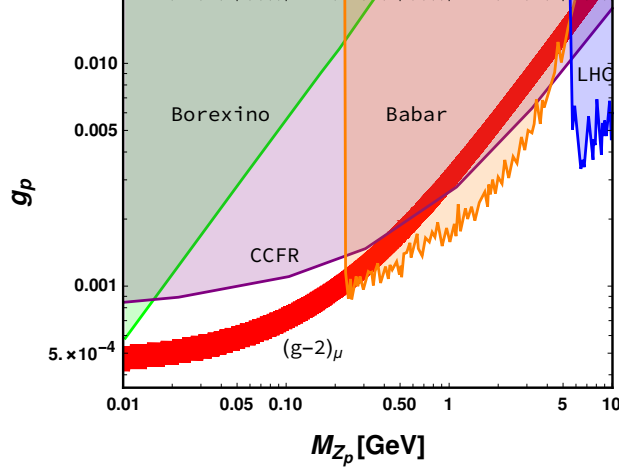


Figure 1. The allowed region that can explain the $(g - 2)_\mu$ anomaly and the excluded region on $M_{Z_p} - g_p$ from different experiments: the green (orange, blue, purple) region is excluded by the Borexino (BABAR, LHC, CCFC). The red region is the parameter satisfying $(g - 2)_\mu$ anomaly [44].

4 Dark matter from leptogenesis

In this section, we consider dark matter relic density as well as leptogenesis in the model. According to Eq. 2.4, v_b and q are related by a pair of $M_{Z_p} - g_p$, which are constrained by the $(g - 2)_\mu$ anomaly. On the other hand, v_b can determine right-handed neutrino mass scale while q corresponds to $U(1)_{L_\mu - L_\tau}$ charge of N_μ which is also related with dark matter. M_{Z_p} and g_p make little difference on our result in this work, therefore we choose $M_{Z_p} = 0.2$ GeV and $g_p = 0.001$ in the following discussion for simplicity, which satisfies $(g - 2)_\mu$ anomaly as well as other collider experiment constraints. The scalar-DM couplings are fine-tuned to be negligible and the gauge-portal channels related to dark matter are highly suppressed due to the choice of the tiny charge q . Therefore, dark matter relic density mainly depends on the scatter processes of $N_{\tau(\mu)} N_{\tau(\mu)} \rightarrow \phi_{dm} \phi_{dm}$. For simplicity, we focus on the case of N_τ , which also plays an important role in leptogenesis¹, and the dominant process related to dark matter relic density is the t-channel interaction of $N_\tau N_\tau \rightarrow \phi_{dm} \phi_{dm}$ according to Fig. 2. There exist couplings of dark matter with other particles in the model, which make the scalar field ϕ_{dm} unstable since ϕ_{dm} can decay into these particles. To make sure the scalar ϕ_{dm} is the dark matter, the lifetime of ϕ_{dm} should be longer than $10^{27} s$, or equivalently $\Gamma_{\phi_{dm}} \leq 6.6 \times 10^{-52}$ GeV in terms of decay width [80]. In the model, we have two possible decay processes related to dark matter. Firstly, the decay channels such as $\phi_{dm} \rightarrow N_\tau N_\tau$ are kinetically forbidden because ϕ_{dm} mass is much smaller than the heavy right-handed neutrinos. Then, we have couplings of dark matter

with light neutrinos due to the heavy-light neutrino mixing, and the lifetime of dark matter is determined by y_{st} and the mixing angle, where the mixing angle is highly suppressed by the right-handed neutrino mass.

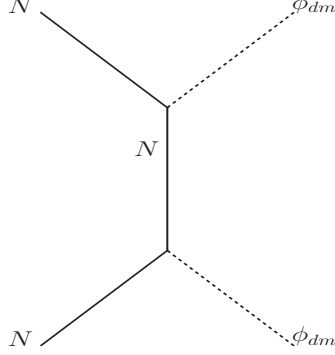


Figure 2. Processes related with the production of dark matter.

4.1 Leptogenesis

In this part, we consider leptogenesis arising from the out-of-equilibrium decays of the heavy right-handed neutrinos in the model. The generated (B-L) asymmetry can be converted into the baryon asymmetry via the sphaleron processes [81, 82], which are active between temperatures of 10^{12} GeV to 100 GeV in the early Universe. The relevant Yukawa matrix for leptogenesis in the model can be identified by [64]

$$y = \begin{pmatrix} y_{De}V_{11} & y_{De}V_{12} & y_{De}V_{13} \\ y_{D\mu}V_{21} & y_{D\mu}V_{22} & y_{D\mu}V_{23} \\ y_{D\tau}V_{31} & y_{D\tau}V_{32} & y_{D\tau}V_{33} \end{pmatrix} \quad (4.1)$$

where V_{ij} are the elements of the matrix V which diagonalizes M_R

$$\text{diag}(M_1, M_2, M_3) = V^\dagger M_R V^*. \quad (4.2)$$

The light neutrino mass matrix poses no special structure and in this work the neutrino mass is fit with the current experiment data. In this part, we choose the following value of M_R in the unit of GeV to fit the proper light neutrino mass.

$$M_R = 10^{10} \times \begin{pmatrix} -7.43984 + 0.134391i & -0.963963 + 0.592564i & -0.829834 - 0.670913i \\ -0.963963 + 0.592564i & -4.92313 + 0.118174i & -0.518899 + 0.0157258i \\ -0.829834 - 0.670913i & -0.518899 + 0.0157258i & -4.74867 - 0.196062i \end{pmatrix} \quad (4.3)$$

where we have set $y_{De} = -0.02$, $y_{D\mu} = 0.02$, $y_{D\tau} = -0.02$ and $v_0 = 200$ GeV. In addition, one can give the elements of V numerically via the values of M_R ,

$$V = \begin{pmatrix} 0.868993 & -0.339967 - 0.244011i & -0.287073 + 0.248069i \\ 0.338398 - 0.142866i & 0.0954554 + 0.161961i & 0.872793 \\ 0.270087 + 0.192304i & 0.888559 & -0.271721 - 0.143009i \end{pmatrix} \quad (4.4)$$

¹Contribution of N_μ to the leptogenesis can be negligible when N_μ mass is much heavier than N_τ .

so the matrix y can be given explicitly by,

$$y = \begin{pmatrix} -2.457988 & 0.961572 + 0.690168i & 0.811966 - 0.701645i \\ 0.685471 - 0.289394i & 0.193358 + 0.328074i & 1.76796 \\ -0.547097 - 0.389539i & -1.7999 & 0.550407 + 0.289685i \end{pmatrix} \quad (4.5)$$

For convenience, we represent N_τ with N in the following discussion. The reaction density for decay is given by,

$$\gamma_D(z) = \frac{m_N^3}{z\pi^2} K_1(z) \Gamma_N \quad (4.6)$$

where $K_1(x)$ is the first kind Bessel function, $z = m_N/T$ with T being temperature, and Γ_N is the decay width of N .

To simplify the discussion, we consider dark matter relic density generated by only N so that we fix y_{sm} to be negligible. We also set the mass of N to be the lightest among the three heavy right-handed neutrinos. We consider dark matter relic density mainly arising from the process of $NN \rightarrow \phi_{dm}\phi_{dm}$ in Fig. 2 during leptogenesis, the reduced cross-section of $NN \rightarrow \phi_{dm}\phi_{dm}$ can be given by [83],

$$\hat{\sigma}(x) = \frac{y_{st}^4}{16\pi} (-2\beta_H(x) + \frac{4\beta_H(x)(r_H - 4)^2}{x^2\beta_H(x)^2 - (x - 2r_H)^2} - \frac{x^2 - 4(r_H - 4)x + 2(r_H - 4)(3r_H + 4)}{x(x - 2r_H)}) \log \frac{(1 - \beta_H(x))x - 2r_H}{(1 + \beta_H(x))x - 2r_H} \quad (4.7)$$

where

$$x = \frac{s_s}{m_N^2}, \quad r_H = \frac{m_{\phi_{dm}}^2}{m_N^2}, \quad \beta_H(x) = \sqrt{(1 - 4/x)(1 - 4r_H/x)} \quad (4.8)$$

and s_s being the squared center-of-mass energy. The reaction density for the process is given by [84],

$$\gamma(z) = \frac{m_N^4}{64\pi^4 z} \int_4^\infty \hat{\sigma}(\omega) \sqrt{\omega} K_1(z\sqrt{\omega}). \quad (4.9)$$

The Boltzmann equations to describe abundance Y_N , dark matter abundance Y_{dm} and lepton asymmetry Y_{B-L} are given as followed in our model [85],

$$\frac{s_N H_N}{z^4} Y'_N = -(\frac{Y_N(z)}{Y_{Neq}(z)} - 1) \gamma_D(z) - \frac{Y_N(z)^2}{Y_{Neq}(z)^2} 2\gamma(z) \quad (4.10)$$

$$\frac{s_N H_N}{z^4} Y'_{dm} = \frac{Y_N(z)^2}{Y_{Neq}(z)^2} 2\gamma(z) \quad (4.11)$$

$$\frac{s_N H_N}{z^4} Y'_{B-L} = -(\frac{1}{2} \frac{Y_{B-L}(z)}{Y_{leq}}) + \epsilon (\frac{Y_N(z)}{Y_{Neq}(z)} - 1) \gamma_D(z) - \Delta W Y_{B-L} \quad (4.12)$$

where ϵ is the CP asymmetry parameter. About quantities in the above three equations, we have,

$$s_N = \frac{2\pi^2}{45} g_* m_N^3, \quad H_N = \frac{1}{2\chi m_{pl}} m_N^2 \quad (4.13)$$

where m_{pl} is the Planck mass with $m_{pl} = 1.22 \times 10^{19}$ GeV, g_* is the effective degrees of freedom with $g_* = 106.75$, and χ is defined by,

$$\chi = \frac{1}{4\pi} \sqrt{\frac{45}{\pi g_*}}, \quad (4.14)$$

Y_{Neq} describes the abundance of N at thermally equilibrium [85],

$$Y_{Neq}(z) = \frac{45z^2}{2\pi^4 g_*} K_2(z) \quad (4.15)$$

where $K_2(z)$ is the second kind Bessel function. Y_{leq} describes lepton abundance at thermal equilibrium,

$$Y_{leq} = \frac{6}{s_N} \frac{m_N^3 \xi(3)}{4\pi^2} \quad (4.16)$$

where $\xi(x)$ is the Riemann zeta function. According to our model, dark matter production is mainly due to the process $NN \rightarrow \phi_{dm}\phi_{dm}$ during leptogenesis non-thermally, and $Y_{dm} \approx 0$ at early Universe. The cross-section of $f\bar{f} \rightarrow Z_p \rightarrow NN$ is too small and makes little contribution to leptogenesis in the model, where f is the fermion of the model. The term ΔW on the right side of the Boltzmann equation represents the possible scattering processes that wash out the generated $(B - L)$ asymmetry. These scattering washouts include $lW^\pm(Z) \rightarrow NH$, $lZ_p \rightarrow NH$, $lH \rightarrow NW^\pm(Z)$, $lH \rightarrow l^c H^*$ and $lN \rightarrow Z_p H$ according to Ref. [64], where l represents lepton in the model and H corresponds to SM Higgs. In addition, the annihilation of $NN \rightarrow Z_p Z_p$ can also dilute the baryon asymmetry although the process is highly suppressed due to the tiny charge q . More details about these washout terms can be found in Ref. [64]. In this work, such scattering processes can make little difference to leptogenesis due to the tiny $U(1)_{L_\mu - L_\tau}$ charge.

After solving the Boltzmann equations, the lepton asymmetry is converted to the baryon asymmetry through sphaleron transitions with the conversion rate [86]

$$Y_B = -\frac{8N_f + 4N_H}{22N_f + 13N_H} Y_{B-L} = -\frac{8}{23} Y_{B-L} \quad (4.17)$$

where we have $N_f = 3$ as the number of fermion families and $N_H = 2$ as the number of Higgs doublets in our model.

The evolution of Boltzmann equations are given in Fig. 3, where the grey lines correspond to the observed value according to Planck 2018 [3] and the black dashed lines Y_{Bo} in the pictures are the results without dark matter, which are obtained by solving Boltzmann equations of right-handed neutrino. In the first picture we fix $y_{st} = 0.5$ and $m_{\phi_{dm}} = 10^{-4}$ GeV, in the second picture we set $y_{st} = 0.05$ and $m_{\phi_{dm}} = 10^{-4}$ GeV, and in the third one we set $y_{st} = 0.005$ and $m_{\phi_{dm}} = 10^{-2}$ GeV.

According to the reaction rate of $NN \rightarrow \phi_{dm}\phi_{dm}$, dark matter abundance is related to the coupling y_{st} as well as dark matter mass $m_{\phi_{dm}}$. In the first and second pictures of Fig. 3, we have much exceeded Y_B density at $z \approx 0$ compared with the case without dark matter. The reason for the extra Y_B is that too many dark matter particles have

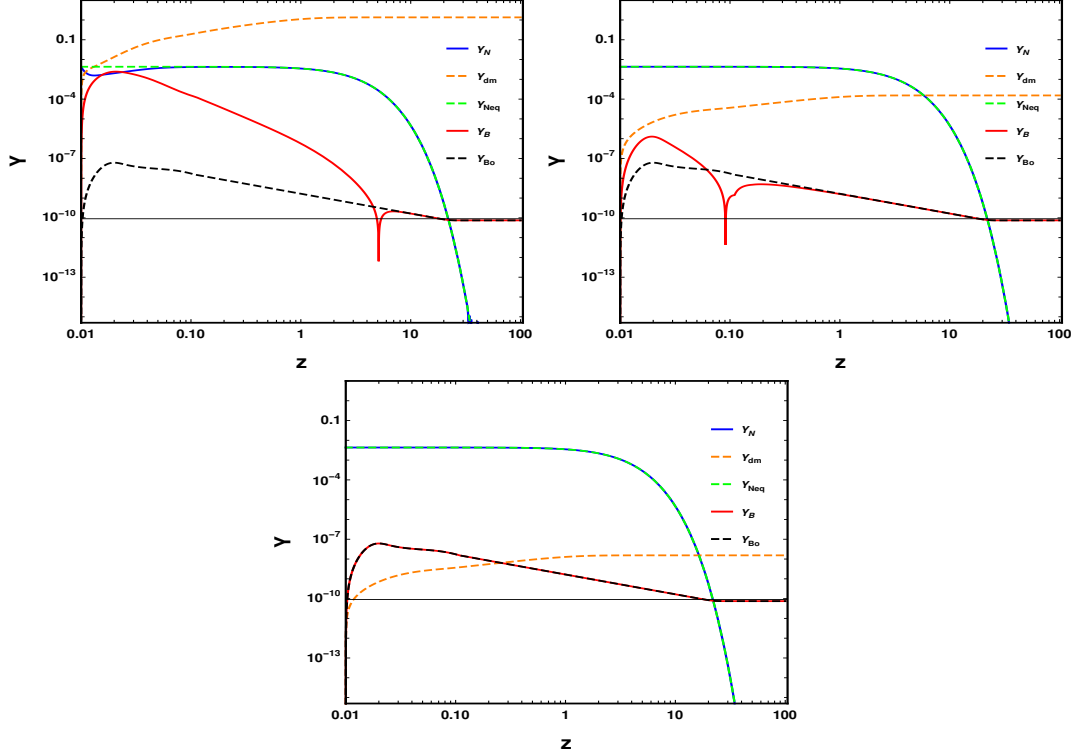


Figure 3. Evolution plots of N abundance Y_N , dark matter abundance Y_{dm} and Baryon asymmetry Y_B , where the black dashed lines Y_{Bo} in all three pictures are the results without dark matter and the grey line corresponds to the observed value according to Planck 2018 [3]. In the top picture we fix $y_{st} = 0.5$ and $m_{\phi_{dm}} = 10^{-4}$ GeV, in the second picture we set $y_{st} = 0.05$ and $m_{\phi_{dm}} = 10^{-4}$ GeV, and in the bottom picture we set $y_{st} = 0.005$ and $m_{\phi_{dm}} = 10^{-2}$ GeV.

been generated so the inverse process is possible. It is obvious that we also have a peak in the first two pictures. The peak in the two pictures arising from the large reaction rate at $z \approx 0.03$ region due to the large y_{st} , such process dilutes the N production so that decreases the $B - L$ asymmetry. For smaller y_{st} , the contribution of the process related to dark matter is much small compared with the N decay and the baryon asymmetry almost coincides with the case without dark matter. The orange lines in Fig. 3 are the evolution of dark matter abundance in our model and for large Yukawa coupling y_{st} , dark matter abundance increases a lot due to the large reaction rate. According to Fig. 3, the Yukawa coupling y_{st} plays an important role in determining dark matter relic density. Moreover, the final baryon symmetries in the three pictures are almost identical to those in the case without dark matter, suggesting that the process of generating dark matter can make little difference on leptogenesis.

4.2 Dark matter

Before discussing the dark matter, we identify the justification for our idea. Firstly, given that dark matter is very light while the mother particle RHNs are very heavy, the huge hierarchy in scales of dark matter production and low energy phenomenology requires

appropriate renormalization group evolution (RGE) in order to make sense of low energy observables. In fact, we obtain the RGEs with the help of SARAH [87], and in Fig. 4 we give the RGEs of g_1, g_2 and g_3 corresponding to the coupling constants of $U(1)_Y$, $SU(2)_W$ and $SU(3)_c$, where we fix $g_p = 0.01, y_{st} = 0.01$, $g_1 = 0.45, g_2 = 0.63$ and $g_3 = 1.04$ for the initial value, and the x-axis corresponds to $lg\Lambda$ with Λ being the energy scale. The results are consistent with the SM case.

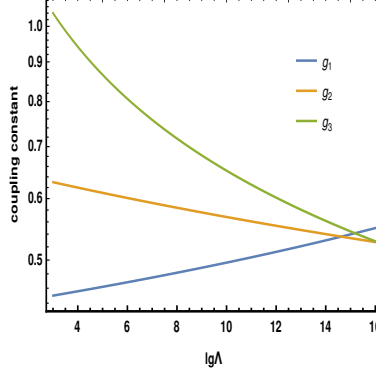


Figure 4. Renormalisation group evolution of g_1, g_2 and g_3 , where we fix $g_p = 0.01, y_{st} = 0.01$, $g_1 = 0.45, g_2 = 0.63$ and $g_3 = 1.04$ for the initial value, the x-axis correspond to $lg\Lambda$ with Λ being the energy scale.

Then, we turn to the non-thermal mechanism to generate dark matter relic density. Firstly, the number density of N is Boltzmann suppressed when the temperature $T < m_N$, which means dark matter is mainly generated in the early universe with $T > m_N$ for the heavy right-handed neutrino mass. Roughly speaking, one can estimate the rate comparison for the process $NN \rightarrow \phi_{dm}\phi_{dm}$ and the expansion rate of the universe $H(T)$ [88] with,

$$H(T) = \left(\frac{4\pi^3 g_*}{45}\right)^{1/2} \frac{T^2}{m_{pl}} = 1.66 \times g_*^{1/2} \frac{T^2}{m_{pl}} \quad (4.18)$$

while the reaction rate Γ can given by

$$\Gamma = n \langle \sigma v \rangle \sim y_{st}^4 T \quad (4.19)$$

where we have used the temperature as the center-of-mass energy. The temperature in thermal equilibrium can be given by:

$$T_{eq} \sim \frac{y_{st}^4 m_{pl}}{1.66 g_*^{1/2}} \quad (4.20)$$

Therefore, dark matter will not be thermalized as long as $T_{eq} < m_N$ and we have

$$y_{st} < \sqrt[4]{\frac{m_N}{m_{pl}}} \quad (4.21)$$

For $m_N > 10^{10}$ GeV, one can estimate y_{st} is approximately smaller than $\mathcal{O}(0.01)$.

As we have discussed above, dark matter abundance in our model is generated with the process $NN \rightarrow \phi_{dm}\phi_{dm}$ during leptogenesis. Current experiment analysis gives dark matter density with [3],

$$\Omega h^2 = 0.120 \pm 0.001 \quad (4.22)$$

and it gives a strict constraint on the parameter space of the dark matter model. The dark matter density expression can be estimated as followed [80],

$$\Omega h^2 \approx \frac{m_{\phi_{dm}} s_0 Y_{dm}(\infty)}{\rho_0/h^2} \quad (4.23)$$

where $s_0 = 2890/\text{cm}^3$ is the entropy density of the present universe, $\rho_c/h^2 = 1.05 \times 10^{-5} \text{ GeVcm}^3$ is the critical density, and $Y_{dm}(\infty) \approx Y_{dm}(m_N/T_{sph})$ with T_{sph} being sphaleron temperature. It is worth stressing that the dominant constraint on the dark matter arising from its free streaming length, which describes the average distance when a particle travels without collisions, and the expression of free streaming length can be given by [34],

$$r_{FS} = \int_{a_{rh}}^{a_{eq}} \frac{\langle v \rangle}{a^2 H(a)} da \approx \frac{a_{NR}}{H_0 \sqrt{\Omega_R}} (0.62 + \log(\frac{a_{eq}}{a_{NR}})) \quad (4.24)$$

where $H(a)$ is the Hubble parameter, $a(t)$ is the FRW scale factor, $\langle v \rangle$ is the averaged velocity of dark matter ϕ_{dm} , a_{eq} and a_{rh} correspond to scale factors in equilibrium and reheating respectively, and a_{NR} is the non-relativistic scale factor. According to [89], we can apply the result of $H_0 = 67.3 \text{ kms}^{-1}\text{Mpc}^{-1}$, $\Omega_R = 9.3 \times 10^{-5}$ and $a_{eq} = 2.9 \times 10^{-4}$. Therefore, the non-relativistic scale factor a_{NR} for the scalar dark matter ϕ_{dm} in our model can be given by [89],

$$a_{NR} = \frac{T_0}{m_{\phi_{dm}}} \left(\frac{g_{*,0}}{g_{*,rh}} \right)^{1/3} K^{-1/2} \quad (4.25)$$

where K is the decay parameter defined by

$$K = \tilde{m}/m_* \quad (4.26)$$

where \tilde{m} and m_* is the effective neutrino mass [84], defined as

$$\tilde{m} = \frac{(y^\dagger y)_{33}}{m_N} \quad (4.27)$$

and m_* is the equilibrium neutrino mass,

$$m_* \approx 1.08 \times 10^{-3} \text{ eV}. \quad (4.28)$$

We can fix $g_{*,0} = 3.91$, $g_{*,rh} = 106.75$ and $T_0 = 2.35 \times 10^{-4} \text{ eV}$, and we can get [90],

$$r_{FS} \approx 5.6 \times 10^{-2} \left(\frac{\text{keV}}{m_{\phi_{dm}}} \right) (50/K)^{1/2} \times (1 + 0.09 \log[(\frac{m_{\phi_{dm}}}{2\text{keV}})(\frac{K}{50})^{1/2}]) \text{ Mpc}.$$

The most strict constraint on r_{FS} results from small structure formation $r_{FS} < 0.1 \text{ Mpc}$ [91]. The case of $r_{FS} > 0.1 \text{ Mpc}$ corresponds to hot DM scenario, while $0.01 \text{ Mpc} < r_{FS} < 0.1 \text{ Mpc}$ and $r_{FS} < 0.01 \text{ Mpc}$ correspond to warm as well as cold DM scenario [92].

4.3 Combined results

In this part, we scan a viable parameter space to discuss the interplay between dark matter and leptogenesis. We choose y_{De} , $y_{D\mu}$, $y_{D\tau}$, v_0 , y_{st} and $m_{\phi_{dm}}$ as inputs. For simplicity, we set $y_{De} = 0.06$ and we scan a viable parameter space with,

$$\begin{aligned} y_{D\mu}, y_{D\tau} &\subseteq [10^{-4}, 1], \\ v_0 &\subseteq [1 \text{ GeV}, 246 \text{ GeV}), \\ m_{\phi_{dm}} &\subseteq [10^{-6} \text{ GeV}, 0.1 \text{ GeV}], \\ y_{st} &\subseteq [10^{-5}, 0.5]. \end{aligned} \quad (4.29)$$

The right-handed neutrino masses are determined by $y_{De, D\mu, D\tau}$ and v_0 , and we bring these parameters in the expression of light neutrino mass and reverse solving M_R matrix so that the eigenvalues of M_R are approximately equal to the right-handed neutrino masses. We restrict the parameter space to satisfy baryon asymmetry and dark matter relic density constraint, where the final baryon asymmetry Y_B is within 3σ range of the observed value with $Y_B \in [8.60, 8.84] \times 10^{-11}$ and $0.11 < \Omega h^2 < 0.13$, and the results are given as followed.

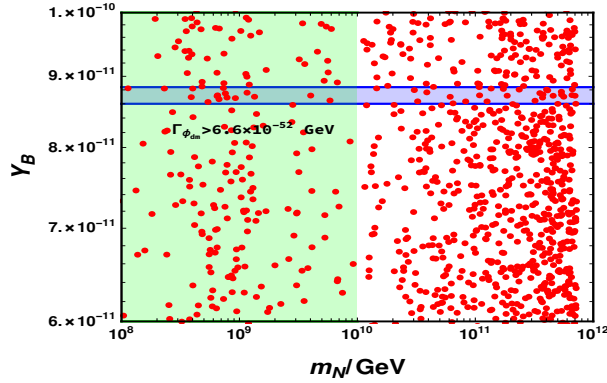


Figure 5. Result of $m_N - Y_B$ within the chosen parameter space, where the blue band corresponds to the final baryon asymmetry within 3σ range of the observed value with $Y_{\Delta B} \in [8.60, 8.84]$. The light-green region is excluded due to the dark matter stability condition.

In Fig. 5, we give the result of $m_N - Y_B$ within the chosen parameter space, where the blue band corresponds to the final baryon asymmetry within 3σ range of the observed value, and the light-green region with $m_N < 10^{10}$ GeV is excluded due to dark matter stability constraint. According to Fig. 5, right-handed neutrino mass is limited within $[10^8 \text{ GeV}, 10^{12} \text{ GeV}]$, and one can always have a successful leptogenesis within the chosen parameter space. However, dark matter can decay into a pair of neutrinos due to the heavy-light neutrino mixing in our model, and a stable dark matter demands $m_N > 10^{10}$ GeV to ensure the mixing angle small enough so that $\Gamma_{\phi_{dm}} < 6.6 \times 10^{-52} \text{ GeV}$ in the case of $y_{st} \subseteq [10^{-5}, 0.5]$. Furthermore, in Fig. 6, we give the contour plot of $v_0 - y_{D\tau}$ satisfying baryon asymmetry and dark matter relic density constraint with $m_N > 10^{10}$ GeV. According to Fig. 6, for $v_0 < 15 \text{ GeV}$, the corresponding right-handed neutrino mass is lighter than 10^{10} GeV regardless of the value of $y_{D\tau}$. Similarly, for $y_{D\tau} < 0.02$,

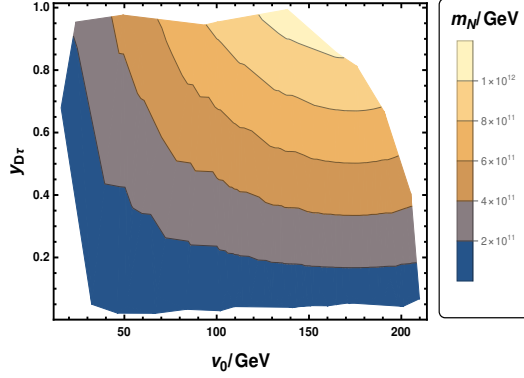


Figure 6. Contour plot of $v_0 - y_{D\tau}$ satisfying baryon asymmetry as well as dark matter relic density constraint, where the x-axis corresponds to v_0 and the y-axis corresponds to $y_{D\tau}$.

right-handed neutrino mass is always lighter than 10^{10} GeV regardless of the value of v_0 . Therefore, a viable parameter space satisfying leptogenesis as well as dark matter stability constraint is $v_0 \geq 15$ GeV and $y_{D\tau} \geq 0.02$ for $m_N > 10^{10}$ GeV.

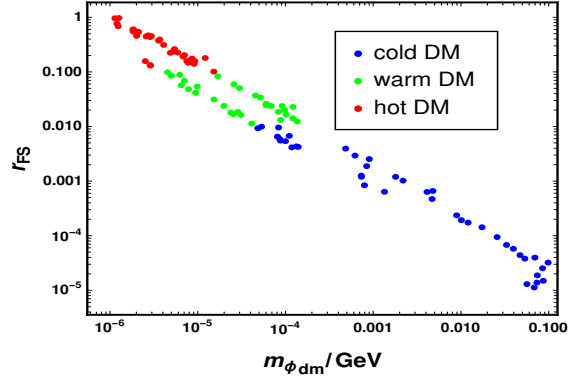


Figure 7. Parameter space of $m_{\phi_{dm}} - r_{FS}$ satisfying baryon asymmetry and dark matter relic density constraint. The blue points correspond to cold dark matter case with $r_{FS} < 0.01$ Mpc, the green points correspond to warm dark matter case with $0.01 \text{ Mpc} < r_{FS} < 0.1$ Mpc, and the red points correspond to hot dark matter case with $r_{FS} > 0.1$ Mpc.

In addition, We can split the viable parameter space into three scenarios as in Fig. 7, according to the constraint from free streaming length r_{FS} . The hot DM scenario is excluded by small structure formation. For warm DM, the possible dark matter mass region is $10^{-5} \text{ GeV} < m_{\phi_{dm}} < 10^{-4} \text{ GeV}$. Meanwhile for cold DM, $10^{-4} \text{ GeV} < m_{\phi_{dm}} < 0.1 \text{ GeV}$ is allowed. Moreover, r_{FS} decreases to about 10^{-5} Mpc in the case of $m_{\phi_{dm}} \sim 0.1 \text{ GeV}$.

We show the parameter space of $m_N - m_{\phi_{dm}}$ in Fig. 8, where the colored points represent parameter space that satisfies the baryon asymmetry constraint as well as dark matter relic density constraint. The heavy right-handed neutrino mass is constrained within $(1 \times 10^{10} \text{ GeV}, 1 \times 10^{12} \text{ GeV})$ while the dark matter mass is $(10^{-6} \text{ GeV}, 0.1 \text{ GeV})$. Moreover, according to Fig. 7, we have different colored points corresponding to hot, warm

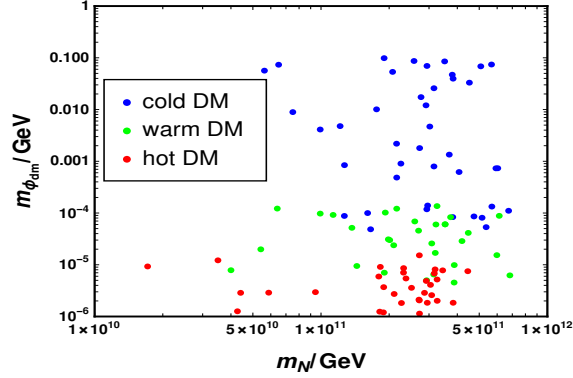


Figure 8. Parameter space of $m_N - m_{\phi_{dm}}$ satisfying baryon asymmetry and dark matter relic density constraint. The blue points correspond to cold dark matter case with $r_{FS} < 0.01$ Mpc, the green points correspond to warm dark matter case with $0.01 \text{ Mpc} < r_{FS} < 0.1 \text{ Mpc}$, and the red points correspond to hot dark matter case with $r_{FS} > 0.1 \text{ Mpc}$.

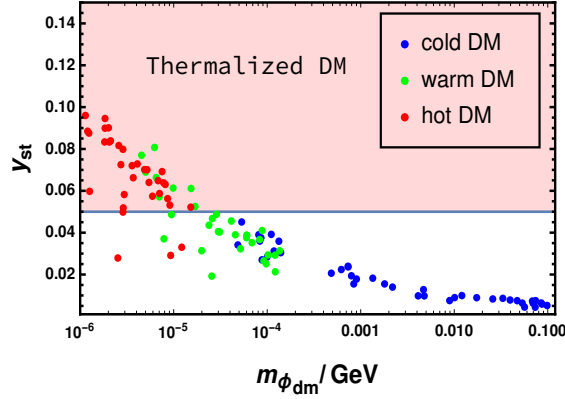


Figure 9. Parameter space for dark matter satisfying baryon asymmetry and relic density constraint. The blue points correspond to cold dark matter case with $r_{FS} < 0.01$ Mpc, the green points correspond to warm dark matter case with $0.01 \text{ Mpc} < r_{FS} < 0.1 \text{ Mpc}$, and the red points correspond to hot dark matter case with $r_{FS} > 0.1 \text{ Mpc}$.

and cold dark matter separately, and three kinds of dark matter are all possible for a certain value of m_N such as $m_N \sim 5 \times 10^{11} \text{ GeV}$. Meanwhile, it is interesting that a heavier m_N often indicates warm or cold DM production. In fact, this is because dark matter is mainly generated during leptogenesis, and heavier m_N means a higher temperature and leptogenesis starts earlier so that dark matter has a long sufficient cooling time.

Dark matter abundance in our model depends on the singlet Yukawa interactions and the dark matter parameter space of $m_{\phi_{dm}} - y_{st}$ is important in our model which can determine the correct relic density. According to Eq. 4.7 and Eq. 4.23, dark matter abundance is approximately proportional to $y_{st}^4 m_{\phi_{dm}}$, which means $m_{\phi_{dm}}$ and y_{st} are stringently restricted by the relic density constraint. In Fig. 9, we give the result of $m_{\phi_{dm}} - y_{st}$ and the colored points correspond to hot, warm and cold DM scenarios respectively. We find a low bound for y_{st} with $y_{st} \geq 0.004$. For smaller y_{st} , dark matter production is not enough

compared with the observed value. Moreover, a lighter dark matter always demands a larger y_{st} so that a larger cross-section is to obtain the correct relic density. It is worth emphasizing that for $y_{st} > 0.05$ the cross-section is so large that dark matter will be thermalized in the late time, which corresponds to the light-red region in Fig. 9. Therefore, a viable parameter space for y_{st} is $0.004 < y_{st} < 0.05$ for the non-thermal production. For the general two-sector leptogenesis scenario, sterile neutrino being dark matter can be generated by the decay of right-handed neutrino via freeze-in mechanism and dark matter abundance depends on the branching ratio of right-handed [34], which corresponds to a wide parameter space. However, in our work, the Yukawa coupling y_{st} related to scalar dark matter production is constrained strictly within a narrow region although dark matter mass $10^{-5} \text{ GeV} < m_{\phi_{dm}} < 0.1 \text{ GeV}$ is allowed. Last but not least, the contribution of dark matter to the final baryon asymmetry can be negligible due to the small cross-section of $NN \rightarrow \phi_{dm}\phi_{dm}$, and the baryon asymmetry constraint does not exclude any parameter. Therefore, we do not need to discuss it elsewhere.

5 summary

Two-sector leptogenesis scenario offers a shared mechanism to unify baryon asymmetry and dark matter problems within a common framework, which can also explain the origin of the tiny neutrino mass problem. In this work, we consider the scalar dark matter model within an extended $L_\mu - L_\tau$ model. Such a model involves neutrino mass, dark matter and can also explain the muon $(g - 2)$ anomaly problem. We discuss the non-thermal dark matter production generated by right-handed neutrinos during the leptogenesis process. The main sector that restricts the stability of dark matter is that dark matter can decay into a pair of neutrinos due to the heavy-light neutrino mixing, which requires the right-handed neutrino N_τ mass larger than 10^{10} GeV . We scan a viable parameter space that satisfies baryon asymmetry and dark matter relic density constraint, where N_τ mass is constrained within the region of $(1 \times 10^{10} \text{ GeV}, 1 \times 10^{12} \text{ GeV})$ consistent with the leptogenesis. On the other hand, N_τ mass is also related to the decay parameter K , which can determine whether dark matter is hot, warm or cold DM and the hot dark matter case is not favored by small structure formation. We found the allowed dark matter mass region is $(10^{-5} \text{ GeV}, 0.1 \text{ GeV})$. Moreover, Yukawa coupling y_{st} related to dark matter can not be necessarily too small and the region to generate the right dark matter relic density is $0.004 < y_{st} < 0.1$. However, for too large y_{st} , one can have the thermalized dark matter case, therefore the right region for y_{st} is $(0.004, 0.05)$.

Acknowledgements

We thank Wei Liu for the early collaboration and useful communications on this work. Hao Sun is supported by the National Natural Science Foundation of China (Grant No.12075043, No.12147205).

References

- [1] Y. Fukuda et al. (Super-Kamiokande), Phys. Rev. Lett. **81**, 1562 (1998), [hep-ex/9807003](#).
- [2] Q. R. Ahmad et al. (SNO), Phys. Rev. Lett. **89**, 011301 (2002), [nucl-ex/0204008](#).
- [3] N. Aghanim et al. (Planck), Astron. Astrophys. **641**, A6 (2020), [Erratum: Astron.Astrophys. 652, C4 (2021)], [1807.06209](#).
- [4] M. Fukugita and T. Yanagida, Phys. Lett. B **174**, 45 (1986).
- [5] P. Minkowski, Phys. Lett. B **67**, 421 (1977).
- [6] R. N. Mohapatra and G. Senjanovic, Phys. Rev. Lett. **44**, 912 (1980).
- [7] M. Gell-Mann, P. Ramond, and R. Slansky, Conf. Proc. C **790927**, 315 (1979), [1306.4669](#).
- [8] J. Schechter and J. W. F. Valle, Phys. Rev. D **22**, 2227 (1980).
- [9] S. L. Glashow, NATO Sci. Ser. B **61**, 687 (1980).
- [10] S. Nussinov, Phys. Lett. B **165**, 55 (1985).
- [11] D. B. Kaplan, Phys. Rev. Lett. **68**, 741 (1992).
- [12] G. R. Farrar and G. Zaharijas, Phys. Rev. Lett. **96**, 041302 (2006), [hep-ph/0510079](#).
- [13] D. Hooper, J. March-Russell, and S. M. West, Phys. Lett. B **605**, 228 (2005), [hep-ph/0410114](#).
- [14] R. Kitano and I. Low, Phys. Rev. D **71**, 023510 (2005), [hep-ph/0411133](#).
- [15] K. Agashe and G. Servant, JCAP **02**, 002 (2005), [hep-ph/0411254](#).
- [16] R. Kitano, H. Murayama, and M. Ratz, Phys. Lett. B **669**, 145 (2008), [0807.4313](#).
- [17] E. Nardi, F. Sannino, and A. Strumia, JCAP **01**, 043 (2009), [0811.4153](#).
- [18] D. E. Kaplan, M. A. Luty, and K. M. Zurek, Phys. Rev. D **79**, 115016 (2009), [0901.4117](#).
- [19] T. Cohen, D. J. Phalen, A. Pierce, and K. M. Zurek, Phys. Rev. D **82**, 056001 (2010), [1005.1655](#).
- [20] L. J. Hall, J. March-Russell, and S. M. West (2010), [1010.0245](#).
- [21] B. Feldstein and A. L. Fitzpatrick, JCAP **09**, 005 (2010), [1003.5662](#).
- [22] J. Shelton and K. M. Zurek, Phys. Rev. D **82**, 123512 (2010), [1008.1997](#).
- [23] H. Davoudiasl, D. E. Morrissey, K. Sigurdson, and S. Tulin, Phys. Rev. Lett. **105**, 211304 (2010), [1008.2399](#).
- [24] N. Haba and S. Matsumoto, Prog. Theor. Phys. **125**, 1311 (2011), [1008.2487](#).
- [25] P.-H. Gu, M. Lindner, U. Sarkar, and X. Zhang, Phys. Rev. D **83**, 055008 (2011), [1009.2690](#).
- [26] M. Blennow, B. Dasgupta, E. Fernandez-Martinez, and N. Rius, JHEP **03**, 014 (2011), [1009.3159](#).
- [27] J. McDonald, Phys. Rev. D **83**, 083509 (2011), [1009.3227](#).
- [28] C. Cheung, G. Elor, L. J. Hall, and P. Kumar, JHEP **03**, 042 (2011), [1010.0022](#).
- [29] C. Cheung, G. Elor, L. J. Hall, and P. Kumar, JHEP **03**, 085 (2011), [1010.0024](#).
- [30] B. Dutta and J. Kumar, Phys. Lett. B **699**, 364 (2011), [1012.1341](#).

- [31] K. M. Zurek, Phys. Rept. **537**, 91 (2014), [1308.0338](#).
- [32] E. Hall, T. Konstandin, R. McGehee, and H. Murayama (2019), [1911.12342](#).
- [33] E. Hall, R. McGehee, H. Murayama, and B. Suter (2021), [2107.03398](#).
- [34] A. Falkowski, E. Kuflik, N. Levi, and T. Volansky, Phys. Rev. D **99**, 015022 (2019), [1712.07652](#).
- [35] A. Falkowski, J. T. Ruderman, and T. Volansky, JHEP **05**, 106 (2011), [1101.4936](#).
- [36] R. Foot, X. G. He, H. Lew, and R. R. Volkas, Phys. Rev. D **50**, 4571 (1994), [hep-ph/9401250](#).
- [37] W. Altmannshofer, C.-Y. Chen, P. S. Bhupal Dev, and A. Soni, Phys. Lett. B **762**, 389 (2016), [1607.06832](#).
- [38] P. Foldenauer and J. Jaeckel, JHEP **05**, 010 (2017), [1612.07789](#).
- [39] S. Baek, N. G. Deshpande, X. G. He, and P. Ko, Phys. Rev. D **64**, 055006 (2001), [hep-ph/0104141](#).
- [40] X. G. He, G. C. Joshi, H. Lew, and R. R. Volkas, Phys. Rev. D **43**, 22 (1991).
- [41] J. Heeck and W. Rodejohann, J. Phys. G **38**, 085005 (2011), [1007.2655](#).
- [42] C.-H. Chen and T. Nomura, Nucl. Phys. B **940**, 292 (2019), [1705.10620](#).
- [43] K. Asai, K. Hamaguchi, and N. Nagata, Eur. Phys. J. C **77**, 763 (2017), [1705.00419](#).
- [44] X. Qi, A. Yang, W. Liu, and H. Sun (2021), [2106.14134](#).
- [45] T. Araki, K. Asai, J. Sato, and T. Shimomura, Phys. Rev. D **100**, 095012 (2019), [1909.08827](#).
- [46] B. Abi et al. (Muon g-2), Phys. Rev. Lett. **126**, 141801 (2021), [2104.03281](#).
- [47] T. Albahri et al. (Muon g-2), Phys. Rev. A **103**, 042208 (2021), [2104.03201](#).
- [48] T. Albahri et al. (Muon g-2), Phys. Rev. D **103**, 072002 (2021), [2104.03247](#).
- [49] P. Foldenauer, Phys. Rev. D **99**, 035007 (2019), [1808.03647](#).
- [50] W. Altmannshofer, S. Gori, S. Profumo, and F. S. Queiroz, JHEP **12**, 106 (2016), [1609.04026](#).
- [51] A. Biswas, S. Choubey, and S. Khan, JHEP **02**, 123 (2017), [1612.03067](#).
- [52] P. Das, M. K. Das, and N. Khan (2021), [2104.03271](#).
- [53] A. Biswas, S. Choubey, and S. Khan, JHEP **09**, 147 (2016), [1608.04194](#).
- [54] K. Deka, S. Sadhukhan, and M. P. Singh (2022), [2203.17122](#).
- [55] F. Costa, S. Khan, and J. Kim (2022), [2202.13126](#).
- [56] N. Okada and O. Seto, Phys. Rev. D **101**, 023522 (2020), [1908.09277](#).
- [57] E. J. Chun and K. Turzyski, Phys. Rev. D **76**, 053008 (2007), [hep-ph/0703070](#).
- [58] B. Adhikary, Phys. Rev. D **74**, 033002 (2006), [hep-ph/0604009](#).
- [59] K. Asai, K. Hamaguchi, N. Nagata, and S.-Y. Tseng, JCAP **11**, 013 (2020), [2005.01039](#).
- [60] P. Bandyopadhyay, E. J. Chun, and R. Mandal, Phys. Rev. D **97**, 015001 (2018), [1707.00874](#).

- [61] P. A. Zyla et al. (Particle Data Group), PTEP **2020**, 083C01 (2020).
- [62] I. Esteban, M. C. Gonzalez-Garcia, A. Hernandez-Cabezudo, M. Maltoni, and T. Schwetz, JHEP **01**, 106 (2019), [1811.05487](#).
- [63] P. F. de Salas, D. V. Forero, S. Gariazzo, P. Martínez-Miravé, O. Mena, C. A. Ternes, M. Tórtola, and J. W. F. Valle, JHEP **02**, 071 (2021), [2006.11237](#).
- [64] D. Borah, A. Dasgupta, and D. Mahanta, Phys. Rev. D **104**, 075006 (2021), [2106.14410](#).
- [65] T. Robens and T. Stefaniak, Eur. Phys. J. C **75**, 104 (2015), [1501.02234](#).
- [66] G. Chalons, D. Lopez-Val, T. Robens, and T. Stefaniak, PoS **ICHEP2016**, 1180 (2016), [1611.03007](#).
- [67] D. López-Val and T. Robens, Phys. Rev. D **90**, 114018 (2014), [1406.1043](#).
- [68] V. Khachatryan et al. (CMS), JHEP **10**, 144 (2015), [1504.00936](#).
- [69] M. J. Strassler and K. M. Zurek, Phys. Lett. B **661**, 263 (2008), [hep-ph/0605193](#).
- [70] B. Pontecorvo, Sov. Phys. JETP **6**, 429 (1957).
- [71] Z. Maki, M. Nakagawa, and S. Sakata, Prog. Theor. Phys. **28**, 870 (1962).
- [72] Z.-z. Xing and Z.-h. Zhao, Rept. Prog. Phys. **84**, 066201 (2021), [2008.12090](#).
- [73] S. Baek and P. Ko, JCAP **10**, 011 (2009), [0811.1646](#).
- [74] E. J. Chun, A. Das, J. Kim, and J. Kim, JHEP **02**, 093 (2019), [Erratum: JHEP 07, 024 (2019)], [1811.04320](#).
- [75] J. P. Lees et al. (BaBar), Phys. Rev. D **94**, 011102 (2016), [1606.03501](#).
- [76] K. Chakraborty, A. Das, S. Goswami, and S. Roy, JHEP **04**, 008 (2022), [2111.08767](#).
- [77] M. Agostini et al. (Borexino), Phys. Rev. D **100**, 082004 (2019), [1707.09279](#).
- [78] M. Abdullah, J. B. Dent, B. Dutta, G. L. Kane, S. Liao, and L. E. Strigari, Phys. Rev. D **98**, 015005 (2018), [1803.01224](#).
- [79] W. Altmannshofer, S. Gori, M. Pospelov, and I. Yavin, Phys. Rev. Lett. **113**, 091801 (2014), [1406.2332](#).
- [80] R. N. Mohapatra and N. Okada, Phys. Rev. D **101**, 115022 (2020), [2005.00365](#).
- [81] N. S. Manton, Phys. Rev. D **28**, 2019 (1983).
- [82] V. A. Kuzmin, V. A. Rubakov, and M. E. Shaposhnikov, Phys. Lett. B **155**, 36 (1985).
- [83] P. S. B. Dev, R. N. Mohapatra, and Y. Zhang, JHEP **03**, 122 (2018), [1711.07634](#).
- [84] M. Plumacher, Z. Phys. C **74**, 549 (1997), [hep-ph/9604229](#).
- [85] S. Davidson, E. Nardi, and Y. Nir, Phys. Rept. **466**, 105 (2008), [0802.2962](#).
- [86] S. Y. Khlebnikov and M. E. Shaposhnikov, Nucl. Phys. B **308**, 885 (1988).
- [87] F. Staub, Comput. Phys. Commun. **185**, 1773 (2014), [1309.7223](#).
- [88] M. C. Bento, O. Bertolami, and R. Rosenfeld, Phys. Lett. B **518**, 276 (2001), [hep-ph/0103340](#).
- [89] P. A. R. Ade et al. (Planck), Astron. Astrophys. **594**, A13 (2016), [1502.01589](#).
- [90] A. Liu, Z.-L. Han, Y. Jin, and F.-X. Yang, Phys. Rev. D **101**, 095005 (2020), [2001.04085](#).

- [91] A. Berlin and N. Blinov, Phys. Rev. Lett. **120**, 021801 (2018), [1706.07046](#).
- [92] A. Merle, V. Niro, and D. Schmidt, JCAP **03**, 028 (2014), [1306.3996](#).